 DOI: 10.1002/masy.200851003

Self-Assembly of Inorganic Nanocrystals: Emergence of a New Physics

M. P. Pileni

In this paper we demonstrate that ordering of nanocrystals on long distance in 3D superlatices called supra crystals permit to emerge of collective intrinsic properties, which was not expected. The shape of the organization at the mesoscopic scale also induces new physical properties.

Keywords: nanocrystals; self-assembly

Introduction

Self-organization of entities in 2D and 3D is one of basic process in nature. Spherical objects like oranges, balls or particles having the same diameter self-organize in compact hexagonal networks (2D) and in 3D ordered structure (fcc or hcp). Concerning particles, opal made of silica particles having few micrometers as diameter self organize in highly ordered structure[1] as atoms in the bulk phase or sodium and chloride ions in NaCl. In some cases it was found these organizations arise specific physical properties due to the ordering.

The first self-assembly of particles having diameter of the few nanometers (<10 nm) was discovered 10 years ago.[2,3] Later on several groups demonstrated that a rather large number of nanocrystals were locally ordered.[2–11] The 3D superlatices were made of few numbers of nanocrystals layers.[7,12,13] To be able to find new physical properties due to the ordering, the nanocrystals have to be ordered at the mesoscopic scale. Relatively very few groups have been able to make 3D superlattices made of several thousand of layers called supra crystals. This was produced for silver,[14,15] CdSe,[3,16] cobalt[17,18] nanocrystals and gold.[19] The collective physical properties of an assembly of nanocrystals[4] are neither those of the isolated particles nor that of the corresponding bulk phase. They could depend on the shape and the nanocrystal assembly at the mesoscopic scale Collective optical[20] and magnetic[21,22] properties due to dipolar interactions are observed when the nanocrystals are organized in 2D superlattices[4]: The optical properties of 5-nm silver nanocrystals organized in hexagonal networks give rise to several plasmon resonances modes, which are attributed to the film anisotropy. In the magnetic properties, the hysteresis loop of nanocrystals is squarer when they are deposited in compact hexagonal networks compared to isolated nanocrystals. The calculated and experimental hysteresis loops for a chain-like structure are squarer than that of a well-ordered array of nanocrystals. The linear chains of nanocrystals behave as homogeneous nanowires.

In the present paper, we demonstrate that the ordering of nanocrystals at the mesoscopic scale, in 3D supra crystals, is not simply an aesthetic arrangement but is in fact a new generation of materials. We first self assembled nanocrystals and we name parameters needed to produce them at mesoscopic scale. Then we describe the various optical, magnetic and crystal growth collective intrinsic properties due to the nanocrystal ordering. We shows that the shape of the mesosctrure of magnetic nanocrystals control the physical properties

Laboratoire LM2N, Université P. et M. Curie (Paris VI), BP 52, 4 Place Jussieu, F - 75231 Paris Cedex 05, France
E-mail: pileni@sri.jussieu.fr

of the nanostructure as oriented anisotropic nanocrystals with same physical behavior but with not the same origin.

Self Organization of Inorganic Nanocrystals

The nanocrystals described below are made in water in oil droplets stabilized by surfactant and called reverse micelles.[23] At the end of the synthesis the nanocrystals are coated with surfactants differing their head polar group.[4] For silver nanocrystals the most used surfactant is dodecanethiol and for cobalt and iron oxide dodecanoic acid. All the experiences described below are down with these two surfactants excepted when it is mentioned in the text. The head polar group of the coating surfactant remains the same, only the chain length and solvent differ. After washing, the coated nanocrystals are dispersed in a given solvent. By deposition of such solution on a substrate the nanocrystals are closed packed in compact hexagonal networks if their size distribution is low enough (inset b Figure 1).[4] Of course, because Vander Walls interactions the ordering is easier for larger nanocrystals. When the

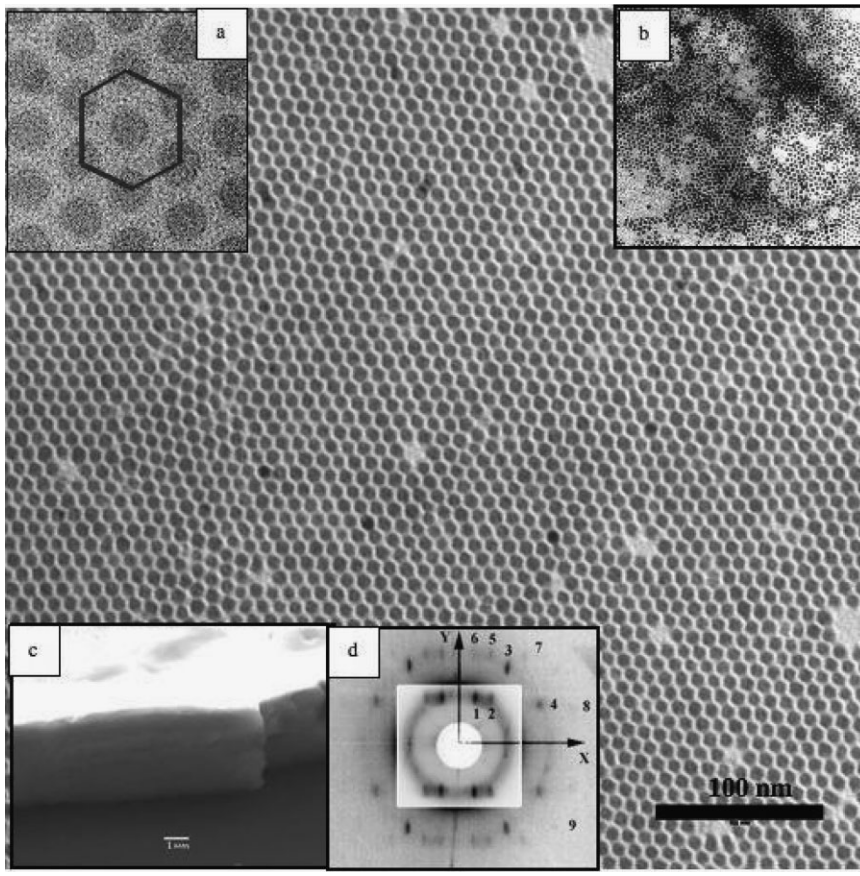

Figure 1.
A monolayer of 7 nm cobalt nanocrystals in very long distance. Inset a: TEM pattern showing that the nanocrystals are organized in hexagonal network. Inset b. The TEM pattern shows no organization in 2D when the nanocrystals do not have similar size. Inset c. SEM pattern of pavement of 7 nm cobalt nanocrystals called supra crystals. Inset d. X Diffraction pattern showing a pure fcc structure.

size distribution is rather large (up to 13%) no compact packing can be obtained (inset d Figure 1). Hence, the size distribution is the keep parameter to produce compact manocrystals order. However it is not the unique one. Particle-particle and particle-substrate interactions[24] play an important role in nanocrystal ordering. Hence, even for very close substrates as amorphous carbon or HOPG (Highly Oriented Pyrolitic Graphite), the ordering is better with silver and cobalt nanocrystals on HOPG than amorphous carbon[17] whereas it is the opposite for Ag_2S.[2]

When cobalt (or silver) nanocrystals are able to self organize in compact hexagonal network on long distance (Figure 1), regular periodic arrangement of nanocrystals in 3D superlattices with more than thousand layer of organized nanocrystals takes place (inset c Figure 1) and form supra crystals[14–18] with the X ray diffraction spots of an ordered in fcc structure (inset d Figure 1).

To determine the influence of the nanocrystal ordering to the physical properties of such assemblies, we need to produce simultaneously, with the same batch of nanocrystals either supra crystals and disordered aggregates i.e to tune the ordering. This is possible by changing the substrate temperature during the deposition process of nanocrystals on the substrate. At low temperature, the deposition gives rise to the formation of a non-homogeneous thin film coexisting with aggregates (Figure 2a). The X-ray diffraction pattern (Figure 2b) has a broad diffuse ring attributed to a disordered material. On increasing the temperature ($10\,^{\circ}C<T<45\,^{\circ}C$), the film morphology changes (Figures 2c, 2e, 2g). On increasing the substrate temperature the pavement area increases and the X-ray diffraction patterns (Figures 2d; 2f; 2h) clearly show the high degree of ordering of the nanocrystals with fcc supra-crystals formation. Thus it is possible to tune the nanocrystal ordering from disordered aggregates to fcc supra crystals. From these results, it is claimed that, even if the same forces are not involved, nanocrystals are able to behave as atoms with formation of either disordered aggregates or crystalline phase as an example amorphous carbon or diamond.

Let us consider nanocrystals having a low dipole interaction with respect to the thermal energy and differing by their average distances from 1.2 nm to 1.6 nm. Interparticle interaction is defined as a sum of the steric repulsion, the dipole-dipole potential and the van der Waals attraction.

Dynamic Brownian simulation taking into account the interparticle interaction shows formation, during the evaporation process, of large spherical aggregates (Figure 3a) when the distance between particles is 1.2 nm whereas they are randomly dispersed (Figure 3b) for a distance of 1.6 nm. Similarly when a magnetic field is applied during the evaporation process, the thick striped structures in the direction of the applied field (Figure 3c) are observed for a distance of 1.2 nm whereas a random nanocrystal organization (Figure 3d) is produced for a 1.6-nm nanocrystal distance. These mesoscopic patterns are explained as follows: when the distances between particles are small enough, aggregates are formed due to the van der Waals forces enhancing considerably the long-range dipolar forces compared to isolated particles; this is accompanied by the formation of a ''macro dipolar moment'' leading to an anisotropic organization of the nanoparticles (Figure 3c). On increasing the particle distance, the van der Waals interactions are too weak to form aggregates and particles behave individually. No aggregation of the particles is observed even when particles are subjected (Figure 3d) or not (Figure 3c) to an applied magnetic field during the evaporation. To improve this model, 10-nm γ-Fe_2O_3 nanocrystals are coated by surfactants with different alkyl chain lengths, the solvent is cyclohexane. With C8, large aggregates of nanocrystals are observed with no applied magnetic field (inset A Figure 3a) whereas the nanocrystals are aligned under an applied field (inset A Figure 3c). With C12, the nanocrystals are dispersed on the substrate with (inset A Figure 3d) and without

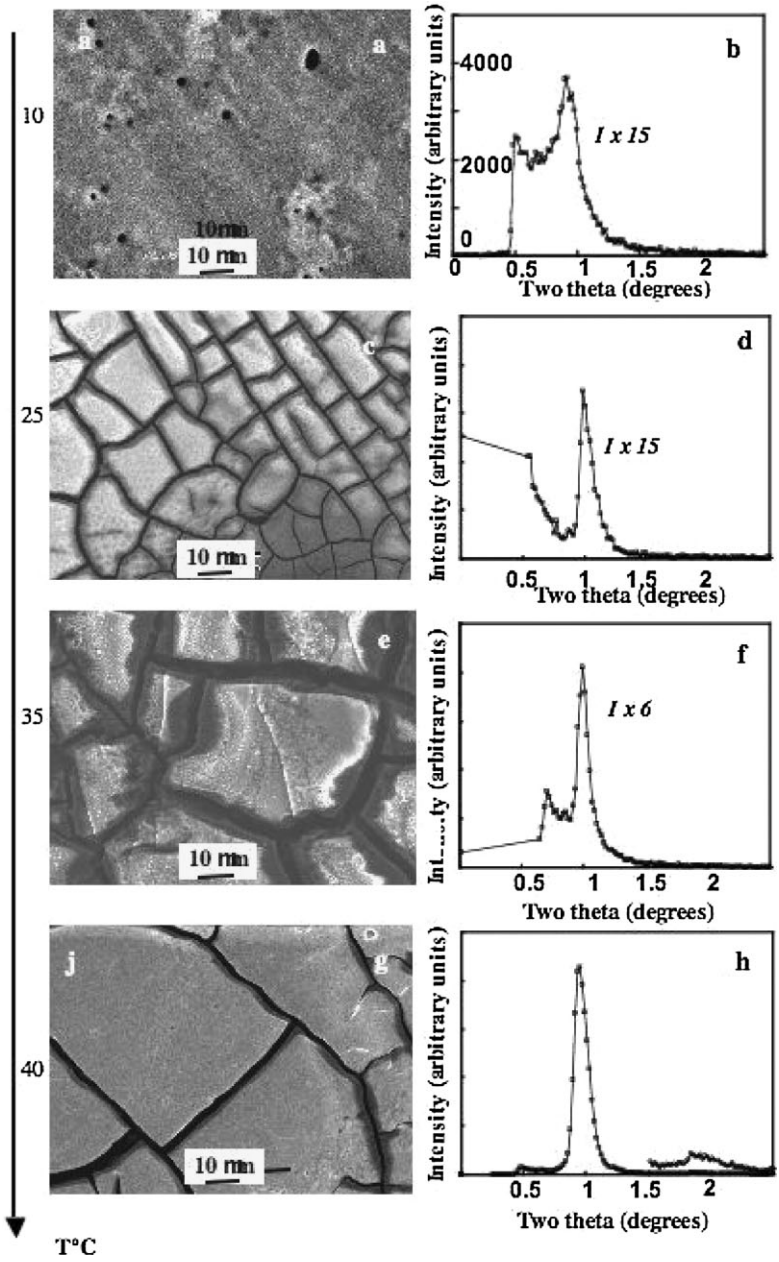

Figure 2.

SEM patterns and X-ray diffraction patterns obtained by deposition of cobalt nanocrystals on HOPG substrate at various temperatures. The different substrate temperatures and corresponding X-ray diffraction patterns are (a, b) $T = 10\,^{\circ}C$, (a, b) $T = 25\,^{\circ}C$, (c d) $T = 35\,^{\circ}C$, (e, f) $T = 45\,^{\circ}C$ (g, h).

(inset A Figure 3b) an applied field. Such behavior is reinforced on increasing the nanocrystals concentration with appearance of rough-surface nanocrystals coated with C8 (inset B Figure 3a) and wires (inset B Figure 3c) in absence and presence of an applied magnetic field, respectively, whereas with C12 a thin film is formed

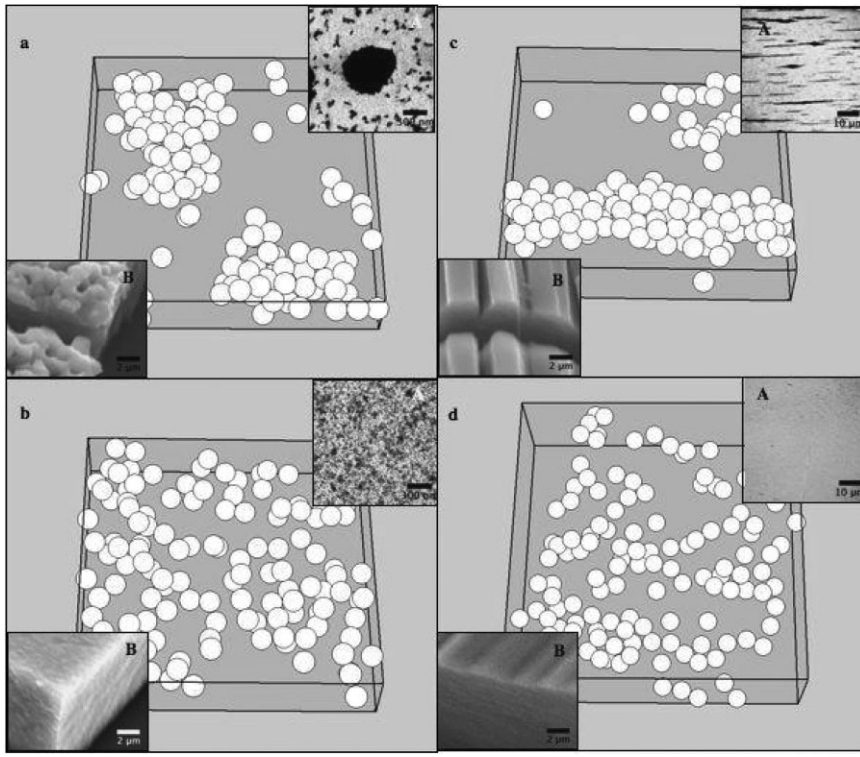

Figure 3.
Snapshots of the configurations by the Brownian dynamics simulations. a, For the coating layer thickness $d = 1.2$ nm (a, c) and $d = 1.6$ nm (b, d) without (a, b) or with (c, d) an applied field. Inset A: TEM patterns obtained with C8 (a, c) and C12 (b, d) without (a, b) or with (c, d) an applied field. Inset B: SEM patterns obtained with C8 (a, c) and C12 (b, d) without (a, b) or with (c, d) an applied field.

(insets B Figures 3b and 3d).[25,26] Hence from the same nanocrystals, it is possible to produce either homogeneous film or nanocrystals wires.[27] This permits to determine whether or not the shape of the mesocopic structure changes the magnetic properties of the assemblies.

Intrinsic Properties due to Long Distance Order of Nanocrystals either in Supra Rystals or in Multiplayers

Vibrational Collective Coherence Properties[28–30]

Silver (or gold) nanoparticles markedly adsorb light by exciting electronic surface plasma dipolar oscillations.[31] This resonance induces intense Raman scattering by the vibration of the nanoparticles. The low frequency Raman spectra of these materials always show a very intense peak close to the Rayleigh line, which is attributed to the excitation of the quadrupolar vibration mode of the nanoparticles via the plasmon-phonon interaction. For disordered aggregates of silver nanocrystals (solid line), the quadrupolar modes appear as sharp intense lines (Figure 4a). For spherical nanocrystals with sizes larger than ~1 nm, the cluster vibrations are described by modelling the nanocrystal with a continuum nanosphere of a diameter D equal to the size of the nanocrystal,[32] and using the longitudinal, v_l, and transversal, v_t,

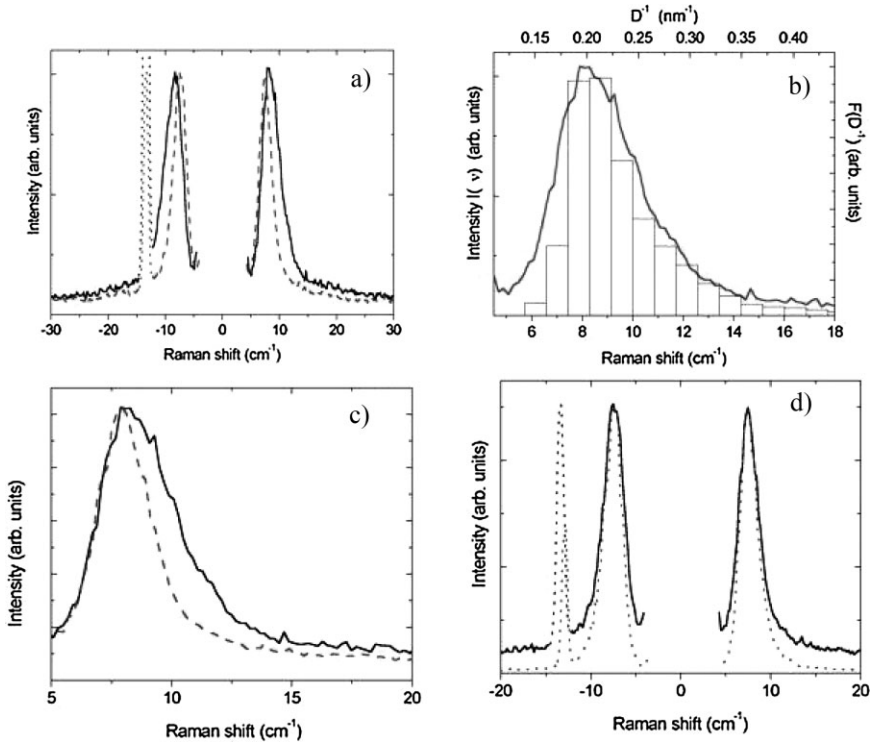

Figure 4.
(a) Raman scattering spectra of 5-nm silver nanocrystals forming either disordered aggregates (black) or a supra-crystal (red). (b) Comparison of the Stokes lineshapes of disordered aggregates. (c) Superposition of Stokes lineshapes after horizontal shifting of disordered aggregates and the supra-crystal. (d) Comparison of the Raman scattered intensity $I^{(3)}(\nu)$ from silver nanocrystals forming small supra-crystals with the profile $\left[I^{(1)}(\nu)\right]^2$ from disordered aggregates of silver nanocrystals.

sound velocities of Ag bulk. The frequencies are given by the following equation:

$$\nu = \frac{S_{\ln} v_t}{D} \quad (1)$$

where S_{ln} depends on the ratio v_l/v_t. Figure 4b shows that the line shape agrees with the inverse size histogram because the intensity of Raman scattering frequency is inversely proportional to the nanocrystal diameter. As already discovered,[33] this indicates that *intra*-nanoparticle coherence, i.e., nanocrystallinity and not *inter*-nanocrystal coherence (or supra-crystallinity).

When the supra crystals are smaller that 1/10 of the excitation wavelength, the Raman peak corresponding to quadrupolar modes is shifted towards a low frequency compared to the disordered aggregate Raman peak (Figure 4a) with a decrease in its width (Figure 4c). This change is due to two effects:

(i) *Effect of the Lorentz field*. The electromagnetic field, that is induced on each nanocrystal by the vibration-fluctuating electric dipoles of the neighboring nanocrystals organized in fcc supra-crystals, changes the nanocrystal polarizability fluctuation.
(ii) *Effect of vibrational coherence*. The van der Waals bonding between thiol chains is sufficient to establish a correlation between the vibrating nanocrystals, so that they vibrate coherently in a supra crystal. The light is scattered by stationary modes in the supra crystal, as by the vibration modes in a molecule. The active vibration modes are

regarded as localized and they are determined only by their symmetry. The intensity of Raman scattering from a supra-crystal, $I^s(\nu)$,[34] is:

$$I^s(\nu) \alpha L^2(\nu)[I^\delta(\nu)]^2 \quad (2)$$

where ν, $[I^d(\nu)]$ and $L(\nu)$ are the frequency, the Raman scattering intensity for a disordered aggregate (without *inter*-nanocrystals) and Lorentz field factor, respectively. The Stokes and anti-Stokes $I^s(\nu)$ profiles are horizontally shifted and vertically rescaled in order to match the peak maxima. The line profile is given by the square of that corresponding to a disordered arrangement of nanocrystals. The narrowed peak of the ''small'' supra-crystals has the same profile as the square of the non-narrowed peak of the ''disordered'' aggregates (Figure 4d). These data clearly indicate inter-nanocrystal coherence inside a fcc supra-crystals.[26–30] Hence, again if the forces involved are not the same, nanocrystals in a supra crystal behave as atoms in a nanocrystal. These coherences could explain the change in the transport properties observed previously with silver nanocrystal self-organizations.[35] These data are confirmed by using a femtosecond reflectivity dynamic with collective vibration of cobalt nanocrystals in supra crystals[36]

Magnetic Intrinsic Collective Properties[27,37–39,40,41]

A general feature characterizing single magnetic nanocrystals is their superparamagnetic behavior. The magnetocrystalline anisotropy energy in axial symmetry depends mainly of the particle volume, V, and its anisotropy constant, K. In the superparamagnetic regime, the anisotropy energy barrier, $E_b = K\,V$, is usually of the same magnitude as the thermal energy. Then the magnetization vector fluctuates among the easy directions of magnetization. This process is called superparamagnetic relaxation. When a magnetic material is subjected to an increasing magnetic field, the spins within the material are aligned with the field. Its magnetization increases and reaches a maximum value called the saturation magnetization, M_s. As the magnitude of the magnetic field decreases, spins cease to be aligned with the field, and the total magnetization decreases. If the magnetic sample is cooled at low temperature (3 K) and then a magnetic field is applied (20Oe) a progressive increase in the magnetization is observed to reach a maximum called blocking temperature, $\mathbf{T_B}$). At higher $\mathbf{T_B}$. value the magnetization of the particle does not depend on temperature and the susceptibility falls This is called zero field cooled (ZFC) magnetization.

Figure 5a shows the ZFC curve normalized to the blocking temperature (T_B) versus temperature curves of both the ordered (red) and disordered (black) supra crystals of 7nm cobalt assemblies. The ZFC peak is significantly narrower for the ordered sample. The width of the ZFC peak is related to the distribution of energy barriers, E_b, in the system: a larger distribution gives a broader peak. The energy barriers involved are the anisotropy energy ($E_a = k_a V$ where k_a is the anisotropy constant and V is the nanoparticle volume) and the dipole-dipole interaction energy which varies with particle distance.[42] Because the ordered and disordered samples are made with the same batch of nanocrystals, this change in width of the ZFC peak is not a consequence of a change in size dispersion of nanoparticles between the two samples or a difference in anisotropy. We therefore explain the difference in the distribution of E_b by the change in the structural environment of the Co nanoparticles. As pointed out dipolar forces have a strong directional dependence and, consequently, dipolar interactions in the assembly should be sensitive to the detailed geometrical arrangement of the nanoparticles. In the supra-crystals, the fcc domains have long coherence lengths and therefore the geometric environment of the nanoparticles is fairly uniform. In the disordered

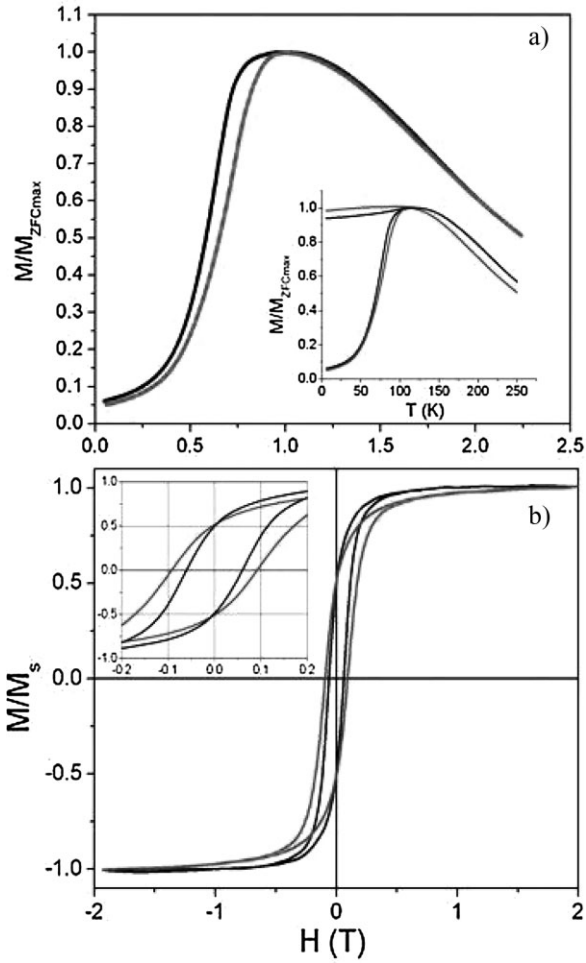

Figure 5.
SEM patterns of supra crystals (a) and disordered aggregates (b). Normalized to the blocking temperature, the ZFC curve of amorphous aggregates (red) and supra crystals (black). corresponding to these configurations calculated for 8-nm cobalt nanocrystals and 0.125 as effective coupling constant.

3D assembly, we have a mixture of many fcc domains characterized by a short coherence length and disordered domains with an irregular stacking periodicity. Therefore, we expect the distribution of $\mathbf{E_{dd}}$ (and hence E_b) in the supra-crystal sample to be lower than in the disordered sample, leading to the observed narrowing of the ZFC peak. We acknowledge that this effect of order is fairly subtle, however, we have found that it is highly reproducible. Figure 5b shows the magnetization versus field curves for the ordered and disordered samples at 5 K. In both cases, saturation is reached at around 1 T and hysteresis is observed. For the ordered sample we find that H_c is larger than for the disordered sample and that the latter saturates at slightly lower fields. This is coherent with a more collective behavior in the supra-crystal compared to the disordered sample. It is reasonable to imagine that the flipping of the spins could require higher fields when the nanocrystals are ordered in a long-range super-lattice compared to the disordered system where we have only very short-range order. The first magnetic intrinsic property due to the ordering is observed.[37–39]

The magnetic properties also markedly differ with the shape of the arrangement of nanocrystal at the mesoscopic structure.[27,41,42] This is demonstrated by using 10-nm γ-Fe_2O_3 nanocrystals, differing by the number of carbon atoms forming the surfactant used to coat them (see above). As observed nanocrystals are able to assemble to form long wires (Figure 6a) or film (Figure 6b) when the length of carbon atoms of the surfactant increases from 8 to 12.

When the direction of applied field is along the long axis (x direction) of the wire the reduced remanance increases compared to that obtained when the applied field is along the short axis whereas it is smaller in the y direction. At the opposite no change in the magnetization is observed when the 10-nm γ-Fe_2O_3 nanocrystals coated with C12 carbon atoms and forming a homogeneous film (Figure 6c). From an energitical point of view we could explain as the orientation of the easy axis of nanocrystals when they are submitted to an applied field. If the easy axis would be oritented the Mossbauer spectrum of such assemblies are expected to change drastically For a disordered aggregates (Figure 6d) and the film (Figure 6f) the Mossbauer relative peaks intensity is, as expected for γ-Fe_2O_3 nanocrystals: 1,2,3 whereas for wires it is 1, 2, 2,14 and 3 (Figure 6e). For a total orientation of the easy axes the relative intensities are expected to be 1,4,3. From hysteresis calculated with a 2.14 relative peak intensity no change in the hysteresis loop cannot be observed.[22] So such slight change in the relative Mossbauer intensity indicates that very few nanocrystals have their easy axis oriented. From the change of the magnetic properties of the assembly

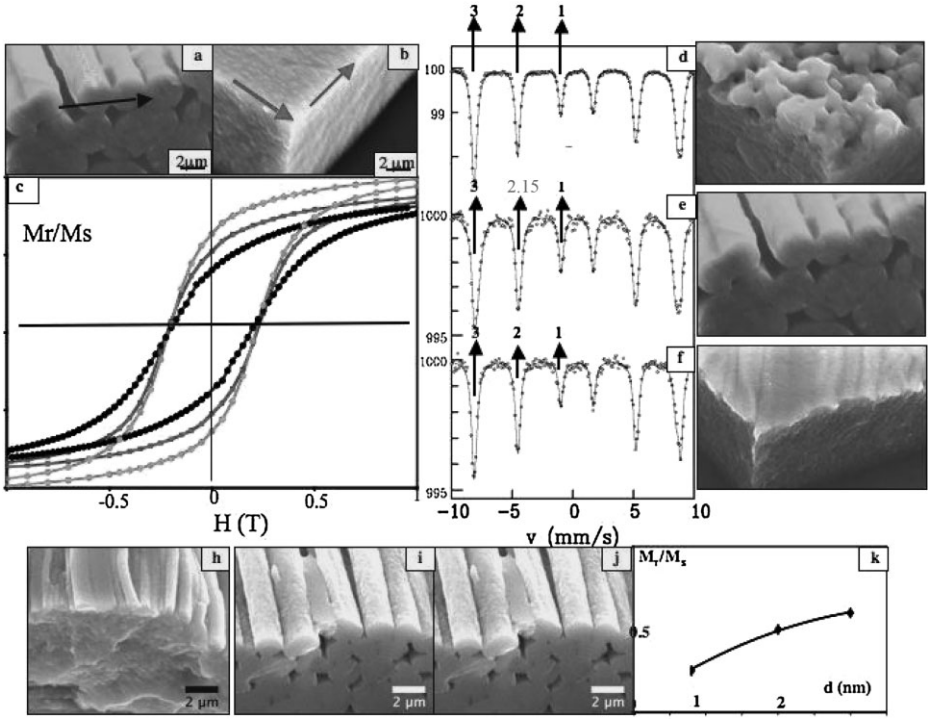

Figure 6.
SEM images of shaped γ-Fe_2O_3 nanocrystals coated either (a) with citrate ions and forming tubes or with decanoic acid and forming a thin film with undulations (b). Magnetization curves at 3 K of tubes recorded either parallel with (green) or perpendicular to (black) and on the film (red) under the two directions.

forming wires (Figure 6a) compared to film (Figure 6b) both made with same batch of nanocrystals permit to claim that change is due to the shape of the mesosocpic strtucture.[41] Note that similar behavior in the magnetic behavior can be observed when the easy axis of the nanocrystals are oriented but the explanation diverges.[40] That means that wires of nanocrystals behave as bulk wires. To confirm such claim the reduced remanance of our wires increases with the size of their widths,as with bulk wires, produced by changing the strength of the applied field used during the deposited process (Figures 6h, 6i, 6j) From that we conclude the change in the magnetic properties is controlled by the shape of the mesoscopic structure. This again can be considered as intrinsic properties.

Epitaxial Orientation due to the Nanocrystals Ordering[43,44]

In the following we use the similar 5nm silver nanocrystals described above. The major differences are the following: the nanocrystals are coated with decanthiol instead of dodecanethiol and dispersed in decane instead of hexane. The TEM grids are covered by HOPG stuck on the grid. In each experiments theTEM grids are immersed in a beaker containing the solution and kept in an oven at 50 °C. One grid is extracted from the oven after decane evaporation (20 hours) whereas the second remains 8 days. At the end of each process the TEM grid is kept at room temperature. The nanocrystals ordering, keeping the same amount of material on the surface, is tuned by slightly change in the deposition mode as described in reference 44 (Figures 7a, 7b and 7c). Hence Figure 7a shows that the nanocrystals are disordered on the substrate as confirmed by the diffuse ring corresponding PS (inset Figure 7a). A higher increase in the ordering is shown on Figure 7b and its inset whereas a long range ordering is observed (Figure 7c). with well defined diffraction peaks (insert Figure 7c). After annealing for 8 days the TEM images show equilateral flat and more or less truncated at the edges triangular shaped particles

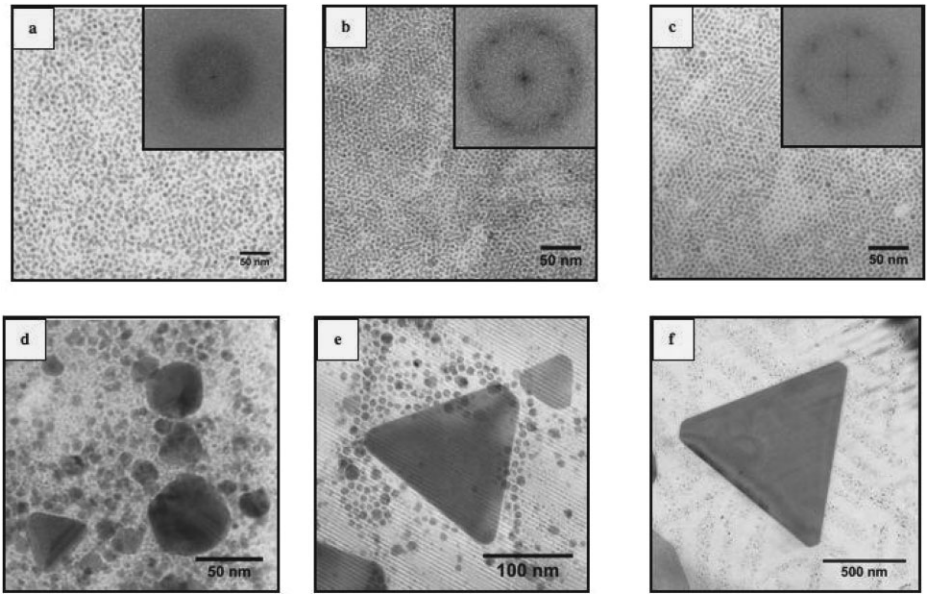

Figure 7.
From a to c: A progressive increase in the nanocrystals ordering by changing the experimental conditions keeping the same amount of material on the substrate. From d to f. A progressive increase in the triangular single crystal size after annealing sample a, b and c respectively (see reference 44).

(Figures 7d, 7e and 7f). Note that the size of equilateral triangles markedly increases with the domain scale of the nanocrystals ordering. Hence rather small triangles (the largest are around 90nm) are produced (Figure 7d) when a local nanocrystals ordering (Figure 7a). On increasing the ordering (Figure 7b), the largest size of the triangle increases to 190nm (Figure 7e) to reach 940nm (Figure 7f) for an ordering on large distance (Figure 7c).

Comparison between dark and bright field TEM image (Figure 8a) indicate a strongly diffracting crystal and high resolution TEM images on the triangles (Figures 8b, 8c, 8d) shows a high crystallinity of the triangles even when at the edges. This indicates that the triangular particles are flat single crystal. When the nanocrystals are ordered on large distance, several triangles are aligned on the substrate (see dotted lines on Figure 8c). An epitaxial orientation on HOPG of triangular nanocrystals is demontrated by TEM diffractions performed, with a reduced diameter of electron beam perpendicular to the flat surface lying on the TEM grid, on several isolated triangular particles.[43,44] From these data it is concluded that single crystals are formed when the silver nanocrystals are ordered and the size of the single crystals is related to the long range organization of particles. The mechanism of epithaxial orientation seems similar to that observe by bulk silver evaporation under (UHV) at high temperature ($\geq$300 °C).[45–53] However the size are much smaller than those obtained on HOPG. Hence self organization of nanocrystals induces formation of triangular single crystals which is favored by epitaxial growth when the substrate is a crystal

Conclusion

In this paper we show some similarity between atoms and nanocrystals. Hence as

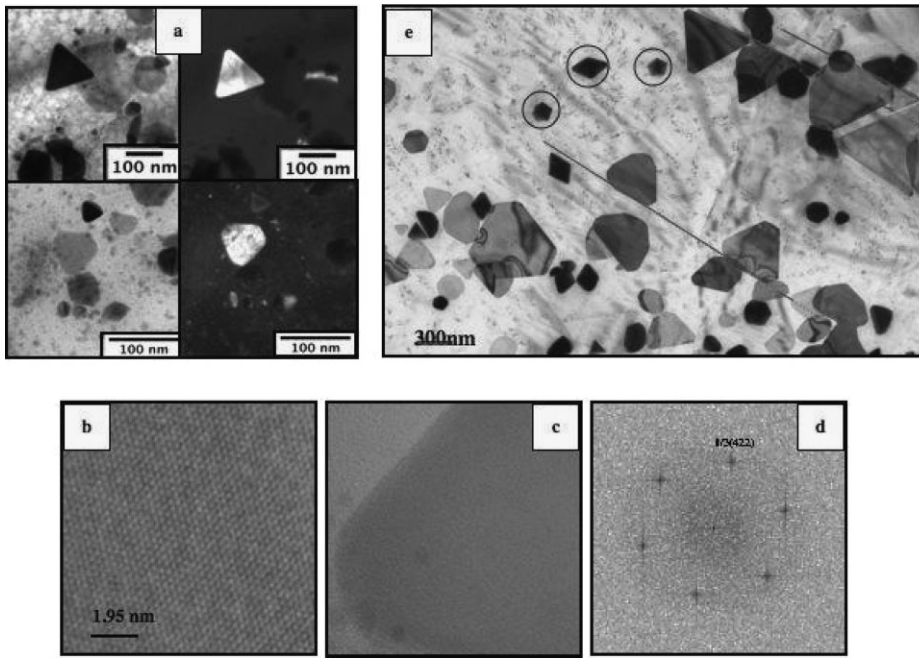

Figure 8.
(a) the dark and bright field images of silver particles. (b and c) HRTEM image of one silver triangular particle anda t its edge. (d) the PS of the HRTEM image.

atoms in a nanocrystals nanocrystals in a supra crystals breath coherently. Similarly the magnetic properties of amorphous aggregates made of nanocrystals and those observed when they are highly ordered in supra crystals are similar to amorphous and crystalline phase of film and/or nanoparticles. Crystal growth observed when nanocrystals are ordered is similar to that observed by evaporation of atoms on a substrate under ultra vacuum.

Acknowledgements: Special thanks are due to my colleages Drs. A. Courty, N. Goubet, A. I. Henry, I. Lisiecki, T. Ngo, D. Parker, J. Richardi.

[1] Color of precious opal J. V. Sanders, *Nature* **1964**, *204*, 1151.
[2] L. Motte, F. Billoudet, M. P. Pileni, *J Phys Chem* **1995**, *99*, 16425.
[3] C. B. Murray, C. R. Kagan, M. G. Bawendi, *Science* **1995**, *270*, 1335.
[4] [4a] M. P. Pileni, *J. Phys. Chem. B.* **2001**, *105*, 3358–3371;[4b] M. P. Pileni, Self-Organization of inorganic nanocrystals. *J. Phys. Cond. Mat.* **2006**, *18*, S65.
[5] M. Brust, D. Bethell, D. J. Schiffrin, C. Kiely, *Adv Mater* **1995**, *9*, 795.
[6] S. A. Harfenist, Z. L. Wang, M. M. Alvarez, I. Vezmar, R. L. Whetten, *J Phys Chem* **1996**, *100*, 13904.
[7] L. Motte, F. Billoudet, E. Lacaze, M. P. Pileni, *Adv. Mat.* **1996**, *8*, 1018.
[8] R. L. Whetten, J. T. Khoury, M. M. Alvarez, S. Murthy, I. Vezmar, Z. L. Wang, P. W. Stephens, C. L. Cleveland, W. D. Luedtke, U. Landman, *Adv. Mat.* **1996**, 428.
[9] S. Murthy, Z. L. Wang, R. L. Whetten, *Philos. Mag. Lett.* **1997**, *75*, 321.
[10] N. A. Kotov, F. C. Meldrum, C. Wu, J. H. Fendler, *J. Phys. Chem.* **1994**, *98*, 2735–2738.
[11] B. A. Korgel, D. Fitzmaurice, *Phys. Rev. B* **1999**, *59*, 14191.
[12] H. Zeng, S. Sun, R. L. Sandstrom, C. B. Murray, *J. Mag. Mag. Mat.* **2003**, *266*, 227.
[13] H. T. Yang, C. M. Shen, Y. K. Su, T. Z. Yang, H. Gao, *J Applied Phys. Letters* **2003**, *82*, 4729.
[14] A. Courty, C. Fermon, M. P. Pileni, *Adv. Mater.* **2001**, *13*, 254.
[15] A. Courty, O. Araspin, C. Fermon, M. P. Pileni, *Langmuir* **2001**, *17*, 1372.
[16] N. Zaitseva, Z. Rong Dai, F. R. Leon, D. Krol, *J. Am. Chem. Soc.* **2005**, 10221.
[17] I. Lisiecki, P. A. Albouy, M. P. Pileni, *Adv. Mater.* **2003**, *15*, 712.
[18] I. Lisiecki, P. A. Albouy, M. P. Pileni, *J. Phys. Chem. B.* **2004**, *108*, 20050.
[19] N. Zeng, J. Fan, G. D. Stucky, *J. Am. Chem. Soc.* **2006**, *128*, 6550.
[20] A. Taleb, C. Petit, M. P. Pileni, *J. Phys. Chem.* **1998**, *102*, 2214.
[21] C. Petit, A. Taleb, M. P. Pileni, *Adv. Mater.* **1998**, *10*, 259.
[22] V. Russier, C. Petit, M. P. Pileni, *J. Applied Physic* **2003**, *93*, 10001.
[23] M. P. Pileni, *J. Phys. Chem.* **1993**, *97*, 6961.
[24] L. Motte, E. Lacaze, M. Maillard, M. P. Pileni, *Langmuir* **2000**, *16*, 3803.
[25] Y. Lalatonne, J. Richardi, M. P. Pileni, *Nature Materials* **2004**, *3*, 121.
[26] Y. Lalatonne, L. Motte, J. Richardi, M. P. Pileni, *Phys. Rev. E 71*, **2005**, 11404.
[27] A. T. Ngo, M. P. Pileni, *Adv. Mater. 12*, **2000**, 276.
[28] A. Courty, A. Mermet, P. A. Albouy, E. Duval, M. P. Pileni, Self-organized Ag-nanocrystals in fcc "supra" crystals: Vibrational Coherence Nature material **2005**, 4, 395–400.
[29] A. Courty, P. A. Albouy, A. Mermet, P. A. Albouy, E. Duval, M. P. Pileni, *J. Phys. Chem.* **2005**, *109*, 21159.
[30] E. Duval, A. Mermet, A. Courty, P. A. Albouy, M. P. Pileni, *Phys. Rev. B.* **2005**, *72*, 85439.
[31] B. Palpant, H. Portales, L. Saviot, J. Lermé, B. Prével, M. Pellarin, E. Duval, A. Perez, M. Broyer, *Phys. Rev. B.* **1999**, *60*, 17107–17111.
[32] E. Duval, A. Boukenter, B. Champagnon, *Phys. Rev. Lett.* **1986**, *56*, 2052–2055.
[33] H. Portales, L. Saviot, E. Duval, M. Fujii, S. Hayashi, N. Del Fatti, F. Vallée, *J. Chem. Phys.* **2001**, *115*, 3444.
[34] E. Duval, A. Mermet, A. Courty, P. A. Albouy, Pileni, *Theory Phys. Rev. B.* **2005**, *72*, 85439.
[35] A. Taleb, F. Silly, A. O. Gussev, F. Charra, M. P. Pileni, *Adv. Mater.* **2000**, *12*, 633–637.
[36] I. Lisiecki, V. Halte, C. Petit, M. P. Pileni, J. Y. Bigot, unpublished data.
[37] I. Lisiecki, D. Parker, C. Salzemann, M. P. Pileni, *Chem Mat. 19*, **2007**, 4030.
[38] I. Lisiecki, D. Parker, C. Salzemann, M. P. Pileni, submitted for pubication.
[39] D. Parker, I. Lisiecki, C. Salzemann, M. P. Pileni, Emergence of new collective properties of cobalt nanocrystals ordered in fcc supra-crystals: - Magnetic Investigation. *J. Phys. Chem. C. 111*, **2007**, 9019.
[40] A. T. Ngo, M. P. Pileni, *J. Appl. Physic.* **2002**, *92*, 4649–4652.
[41] Y. Lalatonne, L. Motte, V. Russier, A. T. Ngo, P. Bonville, M. P. Pileni, *J. Phys. Chem. B* **2004**, *108*, 1848–1854.
[42] J. L. Dormann, L. Spinu, E. Tronc, J. P. Jolivet, F. Lucari, F. D'orazio, D. Fiorani, *J. Magn. Magn. Mater.* **1998**, *183*, L255–L260.
[43] A. Courty, A. I. Henry, N. Goubet, M. P. Pileni, *Nature Materials* **2007**, published on line
[44] A. I. Henry, A. Courty, N. Goubet, M. P. Pileni, *J. Phys. Chem. C* in press.

[45] S. Ino, S. Ogawa, *J. Phys. Soc. Jap.* **1967**, *22*, 1365.
[46] J. G. Allpress, J. V. Sanders, *Surf. Sci.* **1967**, *7*, 1.
[47] G. Honjo, K. Yagi, *J. Vac. Sci. Tech.* **1969**, *6*, 576.
[48] K. Yagi, K. Takayanagi, K. Kobayashi, G. Honjo, *J. Cryst. Growth* **1975**, *28*, 117.
[49] M. Barkai, E. Gruenbaum, G. Deutscher, *Thin Solid Films* **1982**, *90*, 85.
[50] K. Heinemann, T. Osaka, H. Poppa, M. Avalos-Borja, *J. Catal.* **1983**, *83*, 61.
[51] N. Doraiswamy, G. Jayaram, L. D. Marks, *Phy. Rev. B* **1995**, *51*, 10167.
[52] A. A. Baski, H. Fuchs, *Surf. Sci.* **1994**, *313*, 275.
[53] C. Chapon, S. Granjeaud, A. Humbert, C. R. Henry, *Eur. Phys. J. AP.* **2001**, *13*, 23.

